DOI: 10.1002/anie.201203993

Controlled Release

Functional Mesoporous Silica Nanoparticles for Photothermal-Controlled Drug Delivery In Vivo**

*Hong Yan, Cathleen Teh, Sivaramapanicker Sreejith, Liangliang Zhu, Anna Kwok, Weiqin Fang, Xing Ma, Kim Truc Nguyen, Vladimir Korzh, and Yanli Zhao**

Functional mesoporous silica nanoparticles (MSNPs) that can be readily modulated by controllable triggers, such as pH value changes,[1] chemical treatments,[2] electrostatic interactions,[3] enzymatic actions,[4] redox changes,[5] and photoirradiation,[6] have been used effectivly for controlled drug delivery. Among these stimulus conditions, photothermal action can be considered a clean source of energy, and photothermal-powered molecular machines can be reversibly operated and do not generate byproducts. Thus, the construction of novel photothermal-powered systems, although challenging, has been sought after by scientists on account of their potential applications in the areas of nanostructured functional materials,[7] molecular switches,[8] molecular logic gates,[9] and molecular wires.[10]

Photo-switchable azobenzene and its derivatives have been widely applied in catalysts,[11] sensors,[12] soft materials,[13] and even in biological systems.[14] Current challenges of using MSNPs as drug carriers for controlled drug delivery include: how to release drugs without the release of the pore-blocking units to avoid side effects from the released pore-blocking units, how to achieve controlled drug release in vivo, and how to improve the efficiency of drug carriers.[15] Considering these factors, biocompatible photothermal-responsive gates linked covalently to the surface of MSNPs are regarded as one of the best approaches for controlled drug delivery. Although light-induced switchable rotaxanes based on the *trans–cis* photoisomerization of an azobenzene dumbbell threaded into the α-cyclodextrin (α-CD) ring have been well investigated,[16] the synthesis and application of photothermal-responsive rotaxane-mechanized MSNPs for controlled drug delivery have not been reported. In this context, the development of a simple, efficient, biocompatible, and remote-controlled MSNP through the use of photothermal-responsive rotaxanes is of considerable significance.

Herein, we report a novel strategy for the preparation of photothermal-responsive rotaxane-functionalized MSNPs and demonstrate this remote-controlled system for in vivo drug release to wild-type, optically transparent zebrafish larvae. In particular, the functional nanoparticles can efficiently deliver curcumin to zebrafish larvae for the treatment of heart failure. The novel MSNPs were functionalized with [2]rotaxanes in which the α-CD ring is threaded with a linear photothermal-responsive azobenzene axle containing a pre-attached stopper at one end (Scheme 1). The stopper unit has two sulfonic groups, further enhancing the solubility of individual nanoparticles in aqueous solution. The α-CD ring in the [2]rotaxane is initially located at the *trans*-azobenzene position, which is somewhat removed from the nanoparticle surface (*trans*-MSNP-1). It moves to the triazole/ethylene glycol position upon the *trans*-to-*cis* photoisomerization of

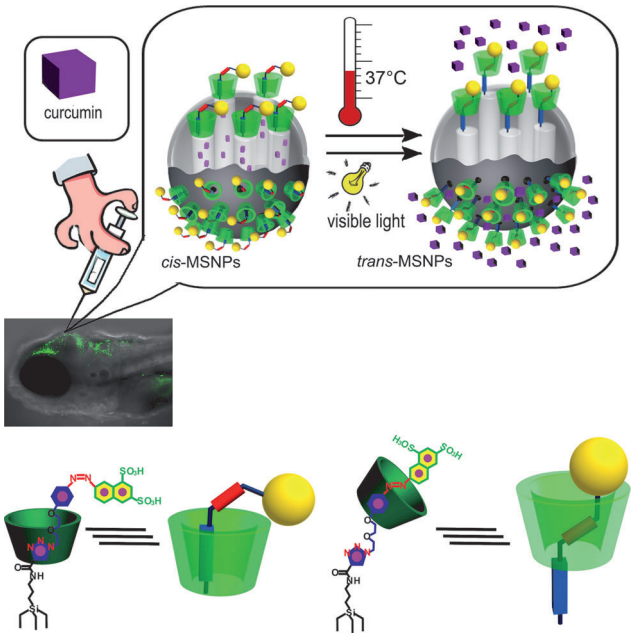

Scheme 1. A graphical representation of the injection of drug-loaded MSNPs into zebrafish larvae for in vivo drug delivery, triggered by either heating or visible light irradiation. MSNPs were functionalized with photothermal-responsive [2]rotaxanes on the surface. The chemical structure of the [2]rotaxane containing the α-CD ring and azobenzene unit is shown.

[*] Dr. H. Yan, Dr. S. Sreejith, Dr. L. L. Zhu, A. Kwok, W. Fang, K. T. Nguyen, Prof. Dr. Y. L. Zhao
Division of Chemistry and Biological Chemistry
School of Physical and Mathematical Sciences
Nanyang Technological University
21 Nanyang Link, 637371, Singapore (Singapore)
E-mail: zhaoyanli@ntu.edu.sg
Homepage: http://www.ntu.edu.sg/home/zhaoyanli/
X. Ma, Prof. Dr. Y. L. Zhao
School of Materials Science and Engineering
Nanyang Technological University (Singapore)
Dr. C. Teh, Prof. Dr. V. Korzh
Laboratory of Fish Development Biology
Institute of Molecular and Cell Biology (Singapore)

[**] We thank the Singapore National Research Foundation Fellowship (NRF2009NRF-RF001-015) and Nanyang Technological University for financial support.

Supporting information for this article (experimental details) is available on the WWW under http://dx.doi.org/10.1002/anie.201203993.

the azobenzene unit under irradiation at 365 nm UV light, physically blocking the pores of the nanoparticles (*cis*-MSNP-1). The *cis*-to-*trans* isomerization of the azobenzene unit upon exposure to visible light or heating causes the α-CD ring to move back to the *trans*-azobenzene position (*trans*-MSNP-1). The back and forth movements of the α-CD ring along the azobenzene axle result in the closing and opening of nanopores, allowing for both drug storage and remote-controlled release.

A convenient and sequential combination of a template-directed synthetic pathway[17] and the copper(I)-catalyzed azide–alkyne cycloaddition (CuAAC) reaction[18] was adopted for the preparation of photothermal-responsive [2]rotaxane attached MSNPs (see Supporting Information, Scheme S3). The azobenzene-containing azide-functionalized thread (**4** in Scheme S1) was stirred with the α-CD ring in aqueous solution for 2 h, forming the pseudo[2]rotaxane. MSNPs functionalized with alkynyl side chains were added to the pseudo[2]rotaxane solution along with $CuSO_4 \cdot 5H_2O$ and sodium ascorbate, and the mixture solution was stirred for 48 h under N_2 atmosphere to give the rotaxane functionalized *trans*-MSNP-1. The α-CD-based [2]rotaxane (not attached to a nanoparticle) and the azobenzene axle-functionalized MSNPs (MSNP-2; without an α-CD ring) were also prepared as references (Scheme S2, S3). Because the α-CD ring has two sides and the dumbbell is nonsymmetrical, two stereoisomers of [2]rotaxane can be formed. For the sake of clarity, we present only one stereoisomer in which the secondary side of the α-CD ring faces the naphthalene stopper.

Detailed investigations to characterize the structures of the pseudo[2]rotaxane (Figure S2) and [2]rotaxane (Figure S3) and to show the photothermal-induced movement of the α-CD ring between the azobenzene moiety and the triazole/ethylene glycol unit in [2]rotaxane were carried out by ^{1}H NMR spectroscopy, ^{1}H ROESY NMR, UV/Vis spectroscopy, CD, and ESI-MS techniques. For the ^{1}H NMR spectroscopy, pseudo[2]rotaxane was prepared by vigorously stirring thread **4** and the α-CD ring in a 1:2 ratio in D_2O (Figure S2). Downfield shifts of protons H^{a-g} on the azobenzene unit in the presence of the α-CD ring clearly indicated that the *trans*-azobenzene moiety of **4** is within the α-CD cavity, forming pseudo[2]rotaxane.[9,19] Irradiation with 365 nm UV light for 30 minuntes formed the *cis* and *trans* isomers in a 2:1 ratio. Similarly, the *trans*-to-*cis* isomerization of the azobenzene unit in [2]rotaxane resulted in shifts of the protons H^{a-g} upon the UV irradiation, and the proton shifts could be recovered with visible light irradiation or heating (Figure S3). The ^{1}H ROESY spectrum of [2]rotaxane showed that the aromatic protons H^f and H^g of the azobenzene unit are spatially close to the internal protons H^5 and H^3 of the α-CD ring (Figure S4).

The UV absorption changes at 370 nm (Figure S5) and CD spectral changes at 360 nm (Figure S6) for the azobenzene unit of the [2]rotaxane upon alternating irradiation with UV and visible light or heating revealed that the switching process of the α-CD ring is reversible and controllable. The formation of pseudo[2]rotaxane and [2]rotaxane was also studied by ESI-MS, giving molecular weights of *m*/*z* 1495.6 ($[M+H]^+$, calcd: 1494.4) for pseudo[2]rotaxane and *m*/*z* 1714.1 ($[M+H]^+$, calcd: 1713.4) for [2]rotaxane (Figure S7).

To determine the association constants (K) the α-CD ring with the different parts of the thread, we prepared two model compounds. One with only an azobenzene moity **S1** and one with a triazole moity **S5** (Scheme S2, S3). The association constants of the azobenzene unit **S1** with α-CD (determined by UV spectral titrations) were $4666\,M^{-1}$ before irradiation with 365 nm UV light and $164\,M^{-1}$ after irradiation (Figure S8). Interestingly, the K of the triazole/ethylene glycol unit **S5** and α-CD was $2600\,M^{-1}$, which lies between the K values of the azobenzene unit **S1** before and after UV light irradiation. This result supports the feasibility of a photothermal-controlled back and forth shuttling of the α-CD ring between the azobenzene and triazole/ethylene glycol units in the [2]rotaxane. Kinetic studies on thermal *cis*-to-*trans* isomerization of [2]rotaxane at different temperatures indicated that the change in absorbance at 370 nm of the azobenzene unit (ΔA_{abs}) after 5 h are 0.067 at 5 °C, 0.086 at 23 °C, 0.101 at 28 °C, and 0.205 at 37 °C (Figure S9). These results demonstrate that a) there is good structural stability of the *cis*-azobenzene axle in the [2]rotaxane at room temperature for light-controlled drug delivery under the experimental time frame and b) it would be feasible to apply *cis*-to-*trans* isomerization of the azobenzene axle at human body temperature (37 °C).

MSNP-1 and reference MSNP-2 were characterized by TEM, powder XRD, and cross-polarization magic angle spinning (CP-MAS) solid-state NMR spectroscopy. High-resolution TEM images of MSNP-1 showed the formation of uniform spherical mesoporous nanoparticles with an average diameter of 60 nm (Figure S10). The N_2 sorption analysis of MSNP-1 revealed a type IV BET (Brunauer–Emmett–Teller) isotherm with a total surface area of $1207\,m^2\,g^{-1}$. A narrow BJH (Barrett–Joyner–Halenda) pore-size distribution was found with an average pore diameter of 3.8 nm. Powder XRD further confirmed the well-ordered structures of the functional MSNPs.

^{13}C CP-MAS solid-state NMR spectroscopy provides solid evidence for the formation of the [2]rotaxane-functionalized silica nanoparticles (Figure S11). A comparison of the solid-state NMR spectra of MSNP-1 and MSNP-2 was carried out. The signals at 10.1, 26.6, 36.7, 42.7, and 48.4 ppm are assigned to aliphatic carbon atoms of the dumbbell component in MSNP-1, and signals at 115.2, 125.2, 129.7, 141.8, 151.7, and 156.8 ppm are attributed to the aromatic carbon atoms of the azobenzene unit in MSNP-1. The signal at 169.7 ppm is characteristic of the carbon atom from a carboxy group (C=O). The grafting of the [2]rotaxanes on the MSNPs was confirmed by a substantial broadening of carbon resonances around 10–70 ppm, which was the result of the carbon atom signals from the α-CD ring.

Figure 1 shows the change in the UV/Vis spectra of photothermal-responsive MSNP-1 in aqueous solution. The nanoparticle solution was stirred during UV and visible light irradiation and heating (65 °C) to avoid precipitation of MSNPs. A temperature of 65 °C was used to accelerate the *cis*-to-*trans* isomerization of the azobenzene unit in this study. In general, the spectral evolution for the *trans*–*cis* isomer-

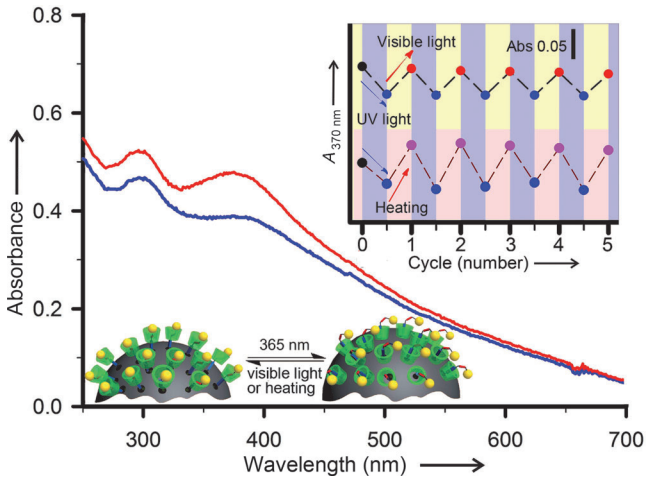

Figure 1. Changes in the UV/Vis absorption spectra of MSNP-1 (1.67 mg mL^{-1}) in aqueous solution after irradiation for 20 minutes with 365 nm UV light (blue) and then after either 15 minutes of visible light irradiation or 30 minutes of heating at 65 °C (red). Inset: the change in absorbance at 370 nm of MSNP-1 as a function of cycles upon either alternating UV and visible light irradiation (top) or alternating UV light irradiation and heating at 65 °C (bottom).

ization of the azobenzene unit had different features (i.e. a decrease of the absorption band at 370 nm by UV light irradiation and an increase of this band by either visible light irradiation or heating to 65 °C), showing the back and forth movements of the α-CD ring along the azobenzene axle on the surface of MSNPs. The azobenzene unit reached its photostationary state within 10 minutes under the UV light irradiation, 15 minutes under visible light irradiation, and 30 minutes with heating (65 °C). The inset plots of Figure 1, show the UV absorbance changes at 370 nm as a function of cycles under either alternating UV and visible light irradiation or alternating UV light irradiation and heating at 65 °C. This result reveals that the photothermal-switching process of the [2]rotaxane on MSNPs is reversible. MSNP-2 also showed a similar *trans–cis* isomerization process upon UV and visible light irradiation (Figure S12).

To investigate the photothermal-induced drug release of MSNP-1, rhodamine B (RhB) and curcumin were employed as cargos. Fluorescent RhB can be considered as a charged drug molecule. Curcumin, the dietary polyphenol derived from turmeric (*Curcuma longa*), has been shown to be a potential therapeutic agent, including as an antitumor, antioxidant, and anti-inflammatory drug.[20] The preparation of either curcumin- or RhB-loaded MSNP-1 is explained in the Supporting Information. When the α-CD ring is located on the *trans*-azobenzene unit of MSNP-1, it does not block the nanopore and thus the drugs can be loaded into the nanopores. Upon irradiation with 365 nm UV light on the drug-loaded MSNP-1, the *trans*-to-*cis* photoisomerization of the azobenzene unit enabled the α-CD ring to shift from the azobenzene unit to the triazole/ethylene glycol position and trapped the drugs within the nanopores. To examine the capping efficiency of the α-CD ring, the release profile of RhB-loaded *trans*-MSNP-1 was recorded in the dark for 24 h. As shown in Figure S13, a negligible amount of RhB (0.001 μmol) leached into the aqueous solution, indicating that MSNP-1 is suitable for drug storage. Next, the release of RhB from MSNP-1 under visible light irradiation was monitored by UV/Vis spectroscopy at 5 °C. The *cis*-to-*trans* photoisomerization of the azobenzene unit under visible light irradiation enabled the α-CD ring to move back to the *trans*-azobenzene position, which led to the opening of the nanopores for drug release.

We then carried out control experiments with nonfunctionalized silica nanoparticles **8** and α-CD-less MSNP-2, to confirm that cargo release depends on the presence of the α-CD ring on MSNPs. First, nanoparticle **8** was loaded with RhB and then washed using the same procedure as above. No obvious changes in both the absorption and emission spectra of **8** upon visible light irradiation were detected, indicating a lack of dye loading into the nanoparticles. Next, the role of the *trans–cis* photoisomerisation of the azobenzene unit without the α-CD ring on the surface of MSNPs was investigated using MSNP-2. After MSNP-2 was loaded with RhB and washed, the absorption intensities were measured both in the dark and after visible light irradiation. In the dark, a gradual absorption enhancement from released RhB (within ten minutes) was observed. As expected, a rapid and uncontrolled release of RhB from MSNP-2 was seen upon the irradiation with visible light (Figure S14). The significant amount of cargo leakage from RhB-loaded MSNP-2, even in the dark, confirms that the azobenzene unit in the absence of an α-CD ring cannot efficiently block the nanopores.

With the design of nanoparticle carriers for in vivo photothermal therapy in mind, the drug-release properties of curcumin-loaded MSNP-1, triggered by visible light or heating, were investigated in solution (Figure 2, Figures S15, S16). The difference in drug release between visible light irradiation and heating was monitored by the time-dependent release from the curcumin-loaded MSNP-1 in

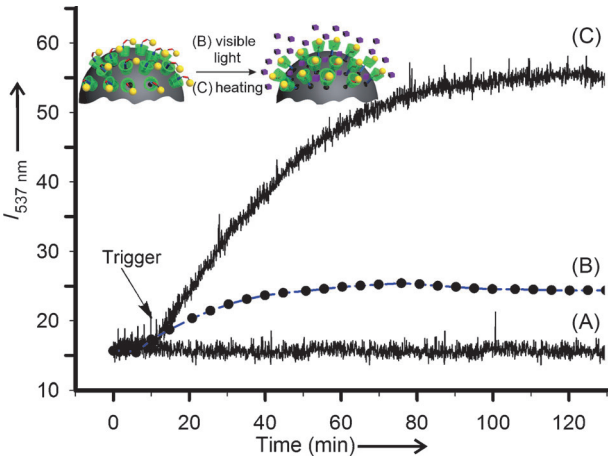

Figure 2. Release experiments of curcumin-loaded MSNP-1 (1.0 mg mL^{-1}) were carried out in H_2O/EtOH (*v*/*v* 4:1), the excitation wavelength (λ_{ex}) is 420 nm, and emission was recorded at 537 nm. Curves (A) and (C) are continuously recorded fluorescence intensity in the dark at 5 °C and 37 °C, respectively, and curve (B) shows the fluorescence intensity every 5 min with visible light irradiation at 5 °C.

solution (H_2O/EtOH *v*/*v* 4:1). In general, the treatment with either visible light or heating on the solution produces distinct release profiles. In Figure 2, the triggered release of fluorescent curcumin by visible light irradiation (B) and heating to 37 °C (C) of the solution of curcumin-loaded MSNP-1 are shown as gradual enhancements of the emission intensities. The curcumin release upon heating appears to be more significant than that from visible light irradiation. Thus, the high releasing efficiency of MSNP-1 controlled by the *cis*-to-*trans* isomerization of the rotaxane unit upon heating makes the nanoparticles an excellent model for thermal-triggered therapy in vivo.

The drug-release efficacy of MSNP-1 was then evaluated in vivo using optically transparent zebrafish larvae. A suspension of curcumin-loaded MSNP-1 (0.1 mg mL^{-1}) was injected into the brain ventricle of five-day-old zebrafish larvae. Curcumin is naturally fluorescent in the visible green spectrum. For photo-induced drug release, we compared the fluorescence intensities between the larvae incubated in the dark at 24 °C (Figure 3C) and the ones that underwent continuous illumination with visible light for a period of one hour at 24 °C (Figure 3D). For thermal-responsive drug release, we compared the fluorescence intensities between the larvae incubated in the dark at 24 °C (Figure 3E) and the ones incubated in the dark at 37 °C for a period of one hour (Figure 3F). The boxed region delimits the zebrafish brain exposed to the curcumin-loaded MSNP-1 and the fluorescence intensity was measured over the boxed area. Curcumin-loaded MSNP-1 showed good drug release when treated with either visible light or heated, both in solution and in vivo (Figure 2, Figure 3, and Figure S16). When compared to the 11.5% reduction in mean fluorescence intensity (Figure 3A,B) in injected larvae that were incubated in the dark, 34.9% and 45.9% reductions in mean fluorescence intensity were observed in vivo after visible light irradiation at 24 °C for one hour and treatment at 37 °C for one hour, respectively. Decreases in the fluorescence intensity of curcumin can be explained by in vivo metabolism of the released curcumin. Importantly, our in vivo results are consistent with the drug release of MSNP-1 in solution, wherein thermally-triggered drug release was more efficient than photo-triggered release. Mean fluorescence intensity changes were calculated from four independent in vivo drug-release experiments using different amounts of curcumin-loaded MSNP-1 (Figure S17).

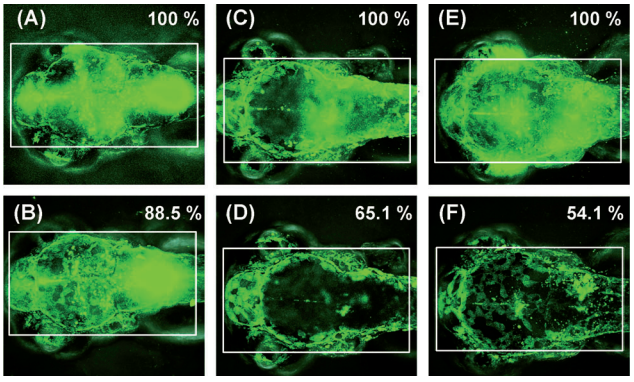

Figure 3. Fluorescence intensities of zebrafish brains microinjected with curcumin-loaded MSNP-1. Fluorescent images were acquired immediately after injection (A) and after 1 h in the dark at 24 °C (B); immediately after injection in the dark (C) and after 1 h with continuous visible light illumination at 24 °C (D), and immediately after injection in the dark at 24 °C (E) and after 1 h in the dark at 37 °C (F). Initial mean fluorescence intensity (A, C, E) was normalized to 100% and the intensity after 1 h (B, D, F) was calculated as a percentage of the initial signal (using Image J software).

One leading mechanism for heart failure is oxidative stress. Curcumin has been found to be an effective therapy of such heart failure, since curcumin is an excellent antioxidant.[20] However, one current issue for curcumin-based therapeutics is their low solubility in aqueous solutions. To investigate the therapeutic potential of curcumin-loaded MSNP-1 on a zebrafish-based heart-failure model, 0.1 mg mL^{-1} of either curcumin suspension or curcumin-loaded MSNP-1 was injected into the venous sinus of zebrafish larvae experiencing heart failure. Ventricle contractility and heartbeat were assessed after incubating the larvae at 37 °C for one hour. Manipulated larvae and wild-type controls were subsequently incubated at 28.5 °C. Figure 4 shows the effect of curcumin toward improving cardiac output

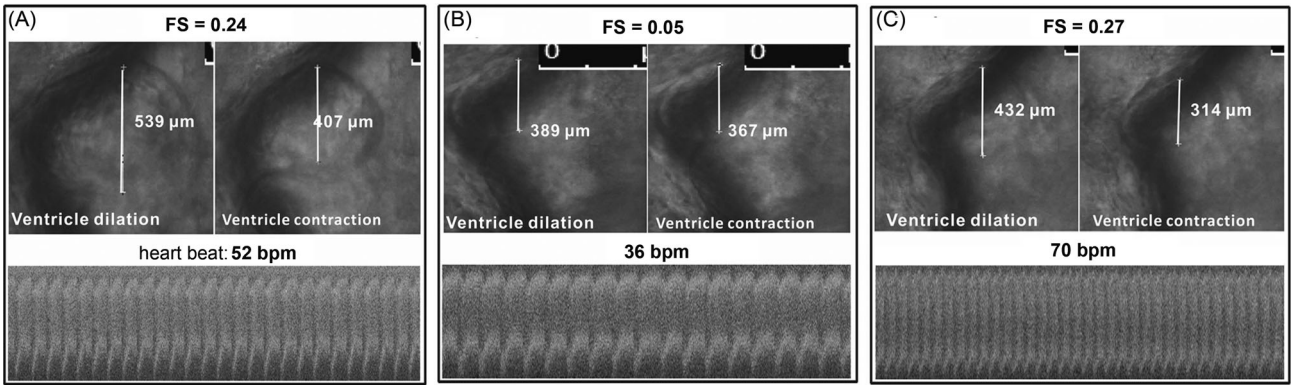

Figure 4. Therapeutic results of curcumin on improving cardiac output of SqKR15 zebrafish larvae experiencing heart failure. Heartbeat of zebrafish experiencing heart failure (A), after microinjection of curcumin into the heart (B), and after microinjection of curcumin-loaded MSNP-1 into the heart (C). Larvae were incubated at 37 °C for 1 h before measuring the ventricle contractility and heartbeat. FS = fractional shortening; bpm = beats per minute.

of SqKR15 zebrafish larvae experiencing heart failure. When compared to untreated larvae experiencing heart failure (Figure 4A) and larvae treated with curcumin alone (Figure 4B), there was a significant improvement in heartbeats per minute (bpm) and contractility (expressed by fractional shortening (FS) that is defined in Figure S18) after treatment with curcumin-loaded MSNP-1 (Figure 4C). The treatment of heart failure by thermal-triggered curcumin-loaded MSNP-1 leads to an FS of 0.27 and 70 bpm, close to the values of normal zebrafish larvae. The heart rate of normal zebrafish larvae ranges from 80 to 160 bpm.[21] This result strongly demonstrates that the curcumin-loaded MSNP-1 can serve as an efficient technique for in vivo drug delivery.

In conclusion, we have developed a novel strategy for the preparation of a new class of photothermal-responsive rotaxane-functionalized mesoporous silica nanoparticles (MSNP-1). The remote-controlled drug release is based on the back and forth movement of the α-CD ring owing to photothermal-induced reversible *trans–cis* isomerization of the azobenzene axle. MSNP-1 has been successfully used for in vivo release of curcumin into five-day-old zebrafish embryos. Efficient thermal-triggered release of curcumin from drug-loaded MSNP-1 was shown to be effective against heart failure in zebrafish larvae and has shed light on future applications of functional nanoparticles. The controllable character of the MSNP-1 system, easily powered by light and temperature, makes it an excellent drug carrier for therapeutic applications. Investigations are ongoing, and we will employ this integrated system to perform targeted photothermal-induced drug release both in vitro and in vivo.

Received: May 23, 2012
Published online: July 6, 2012

Keywords: drug delivery · mesoporous silica nanoparticles · nanoparticles · photothermal switches · zebrafish

[1] a) Y. L. Zhao, Z. X. Li, S. Kabehie, Y. Y. Botros, J. F. Stoddart, J. I. Zink, *J. Am. Chem. Soc.* **2010**, *132*, 13016–13025; b) C. Park, K. Oh, S. C. Lee, C. Kim, *Angew. Chem.* **2007**, *119*, 1477–1479; *Angew. Chem. Int. Ed.* **2007**, *46*, 1455–1457.

[2] C. Y. Lai, B. G. Trewyn, D. M. Jeftinija, K. Jeftinija, S. Xu, S. Jeftinija, V. S. Y. Lin, *J. Am. Chem. Soc.* **2003**, *125*, 4451–4459.

[3] a) A. Baeza, E. Guisasola, E. Ruiz-Hernández, M. Vallet-Regí, *Chem. Mater.* **2012**, *24*, 517–524; b) A. Grattoni, D. Fine, E. Zabre, A. Ziemys, J. Gill, Y. Mackeyev, M. A. Cheney, D. C. Danila, S. Hosali, L. J. Wilson, F. Hussain, M. Ferrari, *ACS Nano* **2011**, *5*, 9382–9391.

[4] a) K. Patel, S. Angelos, W. R. Dichtel, A. Coskun, Y. W. Yang, J. I. Zink, J. F. Stoddart, *J. Am. Chem. Soc.* **2008**, *130*, 2382–2383; b) L. C. Glangchai, M. Caldorera-Moore, L. Shi, K. Roy, *J. Controlled Release* **2008**, *125*, 263–272.

[5] a) T. D. Nguyen, H. R. Tseng, P. C. Celestre, A. H. Flood, Y. Liu, J. F. Stoddart, J. I. Zink, *Proc. Natl. Acad. Sci. USA* **2005**, *102*, 10029–10034; b) T. D. Nguyen, Y. Liu, S. Saha, K. C.-F. Leung, J. F. Stoddart, J. I. Zink, *J. Am. Chem. Soc.* **2007**, *129*, 626–634.

[6] a) N. K. Mal, M. Fujiwara, Y. Tanaka, *Nature* **2003**, *421*, 350–353; b) R. Liu, Y. Zhang, P. Y. Feng, *J. Am. Chem. Soc.* **2009**, *131*, 15128–15129; c) D. P. Ferris, Y. L. Zhao, N. M. Khashab, H. A. Khatib, J. F. Stoddart, J. I. Zink, *J. Am. Chem. Soc.* **2009**, *131*, 1686–1688; d) J. Lu, E. Choi, F. Tamanoi, J. I. Zink, *Small* **2008**, *4*, 421–426; e) S. Angelos, Y. W. Yang, N. M. Khashab, J. F. Stoddart, J. I. Zink, *J. Am. Chem. Soc.* **2009**, *131*, 11344–11346.

[7] a) O. C. Farokhzad, R. Langer, *ACS Nano* **2009**, *3*, 16–20; b) N. Zheng, X. Bu, H. Vu, P. Y. Feng, *Angew. Chem.* **2005**, *117*, 5433–5437; *Angew. Chem. Int. Ed.* **2005**, *44*, 5299–5303.

[8] a) R. A. van Delden, M. K. ter Wiel, M. M. Pollard, J. Vicario, N. Koumura, B. L. Feringa, *Nature* **2005**, *437*, 1337–1340; b) E. M. Pérez, D. T. F. Dryden, D. A. Leigh, G. Teobaldi, F. Zerbetto, *J. Am. Chem. Soc.* **2004**, *126*, 12210–12211.

[9] H. Tian, Q. C. Wang, *Chem. Soc. Rev.* **2006**, *35*, 361–374.

[10] M. Taniguchi, Y. Nojima, K. Yokota, J. Terao, K. Sato, N. Kambe, T. Kawai, *J. Am. Chem. Soc.* **2006**, *128*, 15062–15063.

[11] T. J. Mooibroek, L. Schoon, E. Bouwman, E. Drent, *Chem. Eur. J.* **2011**, *17*, 13318–13333.

[12] X. Cheng, Q. Li, C. Li, J. Qin, Z. Li, *Chem. Eur. J.* **2011**, *17*, 7276–7281.

[13] D. Bléger, Z. Yu, S. Hecht, *Chem. Commun.* **2011**, *47*, 12260–12266.

[14] A. A. Beharry, G. A. Woolley, *Chem. Soc. Rev.* **2011**, *40*, 4422–4437.

[15] M. W. Ambrogio, C. R. Thomas, Y. L. Zhao, J. I. Zink, J. F. Stoddart, *Acc. Chem. Res.* **2011**, *44*, 903–913.

[16] a) H. Murakami, A. Kawabuchi, K. Kotoo, M. Kunitake, N. Nakashima, *J. Am. Chem. Soc.* **1997**, *119*, 7605–7606; b) A. G. Cheetham, M. G. Hutchings, T. D. Claridge, H. L. Anderson, *Angew. Chem.* **2006**, *118*, 1626–1629; *Angew. Chem. Int. Ed.* **2006**, *45*, 1596–1599; c) V. Balzani, A. Credi, M. Venturi, *Chem. Soc. Rev.* **2009**, *38*, 1542–1550.

[17] K. E. Griffiths, J. F. Stoddart, *Pure Appl. Chem.* **2008**, *80*, 485–506.

[18] H. C. Kolb, M. G. Finn, K. B. Sharpless, *Angew. Chem.* **2001**, *113*, 2056–2075; *Angew. Chem. Int. Ed.* **2001**, *40*, 2004–2021.

[19] a) X. Ma, D. Qu, F. Ji, Q. Wang, L. Zhu, Y. Xu, H. Tian, *Chem. Commun.* **2007**, 1409–1411; b) Z. J. Zhang, H. Y. Zhang, H. Wang, Y. Liu, *Angew. Chem.* **2011**, *123*, 11026–11030; *Angew. Chem. Int. Ed.* **2011**, *50*, 10834–10838.

[20] A. Belkacemi, S. Doggui, L. Dao, C. Ramassamy, *Expert Rev. Mol. Med.* **2011**, *13*, e34–49.

[21] C. Teh, D. M. Chudakov, K. L. Poon, I. Z. Mamedov, J. Y. Sek, K. Shidlovsky, S. Lukyanov, V. Korzh, *BMC Dev. Biol.* **2010**, *10*, 110–122.

